Mechanosensing of Integrin α_6 and EGFR Converges at Calpain 2

AD Schwartz[1], CL Hall[1], LE Barney[1], CC Babbitt[2], and SR Peyton[1]*

[1]Department of Chemical Engineering, University of Massachusetts Amherst, Amherst, MA, 01003, USA

[2]Department of Biology, University of Massachusetts Amherst, Amherst, MA, 01003, USA

*Corresponding author: speyton@ecs.umass.edu

Running title: Integrin α_6 and Calpain 2 mechanosensing

Key Words: Biomaterials, Stiffness, Cell Motility, Poly(ethylene glycol), Extracellular Matrix, Laminin

Abstract

Cells sense and respond to mechanical cues from the extracellular matrix (ECM) via integrins. ECM stiffness is known to enhance integrin clustering and response to epidermal growth factor (EGF), but we lack information on when or if these mechanosensitive receptors converge intracellularly. Towards closing this knowledge gap, we combined a biomaterial platform with transcriptomics, molecular biology, and functional assays to link integrin-mediated mechanosensing and epidermal growth factor receptor (EGFR) signaling. We found that high integrin α_6 expression controlled cell adhesion and motility on soft, laminin-coated substrates, and this mimicked the response of cells to EGF stimulation. Signaling pathways downstream of mechanosensitive cell adhesion and motility converged on calpain 2, an intracellular protease important for talin cleavage and focal adhesion turnover. Inhibiting calpain 2 shifted the biphasic dependence of cell migration on substrate stiffness. EGF stimulation enhanced both adhesion and motility on soft substrates, but required the presence of both integrin α_6 and calpain 2. In sum, we identified a new role for integrin α_6 mechanosensing, where high integrin α_6 binding to laminin mimicked the effect of EGF stimulation. Downstream of both integrin α_6 and EGFR, calpain 2 is known to control focal adhesion dynamics and motility, implicating integrin α_6 and calpain 2 as potential targets to inhibit the migration of cancer cells in stiff tumor environments.

Introduction

Carcinoma progression is associated with deposition of ECM that stiffens the local microenvironment [1, 2]. This tissue stiffening results in deposition of additional matrix protein, initiating a positive feedback loop between cells and the evolving stroma [3]. Cells sense and respond to the stiffness of their environment via RhoA GTPase activation, which feeds back to increase cell contractility via activation of myosin light chain kinase [4]. These ECM-driven changes in cytoskeletal tension also regulate motility in a cell-type specific manner [5]. *In vitro*, synthetic biomaterials have revealed that the type of material, stiffness, and biochemical surface modification alter the attachment and motility of cells [6, 7]. We therefore hypothesized that independently tuning stiffness, integrin-binding sites, and chemokinetic factors could reveal new mechanosensitive proteins that drive cell adhesion and motility in different environments.

Several mechanically responsive genes and proteins have been implicated in breast cancer metastasis [8]. For example, extracellular mechanical forces in the tumor microenvironment alter nuclear stiffness and gene expression [9] and activate adhesion proteins, including focal adhesion kinase (FAK) and talin [10-12], leading to increased motility. One class of surface receptors, integrins, translate extracellular forces to downstream signaling cascades in a process called *mechanotransduction*. Increasing substrate stiffness increases integrin binding and clustering, which has implications for several pathways in breast cancer metastasis, including FAK and PI3K signaling [13, 14]. However, most cancer mechanobiology research has focused on collagen- and fibronectin-binding integrins. Integrins that bind to other ECM proteins, such as laminin, have been neglected, despite the prevalence of laminin in the tumor ECM [15, 16].

EGFR has recently emerged as mechanosensitive [17, 18]. The mechanisms of EGFR mechanosensing are unknown, but understanding this process is critically relevant to cancer progression, given the known abundance of EGF in tumors [19] and frequent acquired resistance to EGFR inhibitors [20]. Residues on EGFR can be phosphorylated by $\alpha_V\beta_3$ integrin clustering [21], so we postulated that there could be a role for integrins in facilitating EGFR mechanosensing [22].

To uncover whether such a relationship exists, we created a biomaterial system to identify mechanoresponsive proteins working cooperatively downstream of EGFR phosphorylation and integrin engagement. Through a combination of transcriptomics, molecular biology, and quantification of cell adhesion and motility, we found that the intracellular protease calpain 2 is likely one of these links. Both calpain 2 and integrin α_6 expression had an inverse relationship with ECM stiffness. Engagement of integrin α_6 adhesion mimicked the effect of EGF stimulation in a stiffness-dependent manner. Integrin α_6 can directly associate with EGFR, which increased cell motility via calpain 2. In sum, this study highlights the utility of tunable biomaterials systems to uncover previously unrealized relationships between different classes of proteins in mechanobiology.

Materials and Methods

Cell Culture. All cell culture reagents were purchased from Thermo Fisher Scientific (Waltham, MA) unless otherwise specified. MDA-MB-231 cells were a generous gift from Sallie Schneider at the Pioneer Valley Life Sciences Institute. Highly metastatic and tropic MDA-MB-231 variants were kindly provided by Joan Massagué at the Memorial Sloan Kettering Cancer Center. These cell lines preferentially metastasize to the bone (1833 BoM [23]) brain (831 BrM2a [24]) or lung (4175 LM2 [25]). All cells were cultured in Dulbecco's modified eagle medium (DMEM) with 10% fetal bovine serum (FBS) and 1% penicillin-streptomycin (P/S) at 37°C and 5% CO_2.

Synthesis of Poly(ethylene glycol)-phosphorylcholine (PEG-PC) Gels. PEG-PC gels were formed as previously described [26]. For this application, a 17wt% solution of 2-methacryloyloxyethyl phosphorylcholine (PC) (730114-5g, Sigma Aldrich, St. Louis, MO) in pH 7.4 phosphate buffered saline (PBS) was mixed with varying concentrations of poly(ethylene glycol) dimethacrylate (PEGDMA) (Sigma). This solution was filtered through a 0.22 μm PVDF syringe filter, and excess oxygen was removed by degassing with nitrogen for 30 seconds. 20wt% Irgacure 2959 (BASF, Florham Park, NJ) was dissolved in 70% ethanol and added to the

polymer solution in a ratio of 40 µL Irgacure to 1 mL of polymer solution. 50 µL of this final hydrogel precursor solution was sandwiched between a 3-(trimethoxysilyl)propyl-methacrylate treated 15mm diameter coverslip and an untreated coverslip and UV polymerized for 20 minutes. Gels were swelled in PBS for at least 48 hours before functionalizing the surface using 0.3 mg/mL Sulfo-SANPAH (c1111-100mg, ProteoChem, Hurricane, UT) in 50 mM HEPES buffer at pH 8.5, under UV for 10 minutes. Gels were then flipped onto droplets to achieve a final concentration of either 10 µg cm^{-2} collagen 1 (A1048301, Thermo Fisher Scientific), 10 µg cm^{-2} collagen 1 + 0.5 µg cm^{-2} β_1-chain-containing laminin isoforms (AG56P, Millipore, Billerica, MA), or 10 µg cm^{-2} collagen 1 + 20 ng cm^{-2} EGF (R&D Systems, Minneapolis, MN). Gels were incubated with protein overnight in a hydrated chamber at room temperature, washed in PBS, and sterilized under germicidal UV for 1 hour before cell seeding. For mechanical testing, gels were formed in a cylindrical mold (5µm high, 5µm diameter), allowed to swell for at least 48 hours and compression rheology was performed using an AR2000 (TA Instruments, New Castle, DE), as previously described [26].

RNA-Seq. Total RNA was isolated using Gen Elute mammalian total RNA Miniprep kit (RTN70, Sigma Aldrich). The TruSeq stranded RNA LT kit (15032612, Illumina, San Diego, CA) was used to purify and fragment the mRNA, convert it to cDNA, and barcode and amplify the strands. Quality and length of the inserts was confirmed with an Agilent Genomics 2100 bioanalyzer, followed by single-end 75 bp reads on the MiSeq (Illumina) to generate a complete transcriptome from each sample. Transcripts were aligned to the hg19 human reference genome using the Tuxedo Suite pathway [27-30]. Cufflinks was used to determine statistically significant differential expression of genes ($p<0.05$) [31-33].

qRT-PCR. Total RNA was isolated from 2 biological replicates as previously described [34]. 50 ng cDNA was then amplified using 10 pmol specific primers (Table S1) and the Maxima Sybr green master mix (Thermo Fisher Scientific) on a Rotor-Gene Q thermocycler (Qiagen, Valencia, CA) as follows: 50°C for 2 minutes, 95°C for 10 minutes followed by 45 cycles at 95°C for 10 seconds, 58°C for 30 seconds, and 72°C for 30 seconds. Both β-actin and ribosomal protein S13 were included as reference genes to permit gene expression analysis using the 2^{-ddCt} method.

Cell Adhesion Quantification. MDA-MB-231 cells were seeded at a final density of 5,700 cells cm^{-2}. Cells were either seeded immediately, or pretreated for 30 minutes before seeding with a small molecule ERK inhibitor FR180204 (Sigma Aldrich), calpain inhibitor IV (208724, Millipore), or 100 ng mL^{-1} EGF. The plate was pre-incubated on the Zeiss Axio Observer Z1 microscope (Carl Zeiss AG, Oberkochen, Germany) for 1 hour, then cells were seeded onto gels functionalized with collagen 1, collagen 1 + laminin, or collagen 1 + 20ng cm^{-2} bound EGF and imaging was started within 10 minutes of seeding. Images were taken with a 20x objective every 5 minutes for at least 2 hours. Cells were manually traced using Image J (NIH, Bethesda, MD). N≥ 50 cells per condition.

Cell Migration. Cells were seeded onto gels functionalized with 10 µg cm^{-2} collagen 1 or 10 µg cm^{-2} collagen 1 + 20ng cm^{-2} EGF at a density of 5,700 cells cm^{-2} and allowed to adhere for 24 hours. For inhibitor conditions, cells were treated 2 hours prior to the start of imaging with calpain inhibitor IV, ERK inhibitor FR180204, EGFR-HER2 dual kinase inhibitor (Lapatinib, LC Laboratories, Woburn, MA), or 10 ng mL^{-1} EGF (R&D Systems). Cells were imaged at 15 minute intervals for 12 hours on the Zeiss Axio Observer Z1 microscope (Carl Zeiss AG). N≥ 48 cells per condition were manually tracked using the manual tracking plugin for Image J (NIH, Bethesda, MD).

Generation of ITGA6 and CAPN2 shRNA transduced cells. The shRNA sets specific to human *ITGA6* (Sequence: CCGGCGGATCGAGTTTGAT AACGATCTCGAGATCGTTATCAAACTCGATCCGTTTTTG) and *CAPN2* (sequence: CCGGCAGGAACTACCCGAACACATTCTCGAGAATGTGTTCGGGTAGTTCCTGTTTTTG) were purchased from Sigma-Aldrich (St. Louis, MO). Plasmids (in pLKO.1-puro) were packaged into virus particles according to manufacturer's instructions and used to transduce MDA-231-luciferase cells. Stable pools were selected using 1 mg ml^{-1} puromycin (Invivogen, San Diego, CA). Cells transduced with a non-targeting shRNA served as a control.

Immunofluorescent Staining and Imaging. 28,500 cells cm^{-2} were seeded and fixed at 24 hours in 4% formaldehyde. Cells were permeabilized in Tris-Buffered Saline (TBS) with 0.5% Triton-X and washed 3 times

in TBS with 0.1% Triton-X (TBS-T). Blocking was done for 1 hour at room temperature in TBS-T + 2%w/v Bovine serum albumin (BSA, Sigma Aldrich) (Abdil). Cells were then incubated in primary antibody in Abdil for 1 hour at room temperature using 1 or more of the following antibodies; vinculin (V9264-200UL, 1:200, Sigma Aldrich), pEGFR-Y1068 (ab32430, 1:200, Abcam, Cambridge, MA), total EGFR (D38B1, 1:200, Cell Signaling, Danvers, MA), integrin α_6 (ab134565, 1:200, Abcam), integrin α_3 (ab131055, 1:200, Abcam), ERK (ab54230, 1:200, Abcam), calpain 2 (MABT505, 1:200, Millipore), or phalloidin 647 (A22287, Thermo Fisher Scientific). For insoluble fractions, cells were permeabilized in cold Tris-Buffered Saline (TBS) with 0.5% Triton-X at 4°C for 1 minute prior to fixing. For immunofluorescent imaging of ECM proteins, cells were fixed at 24 hours (57,000 cells cm^{-2}) or 6 days (11,400 cells cm^{-2}) before staining with a pan-laminin antibody (ab11575, 1:100, Abcam) and collagen 1 antibody (ab6308, 1:200, Abcam). Molecular Probes secondary antibodies were used at a 1:500 dilution (goat anti-mouse 555 (A21422) and goat anti-rabbit 647 (A21244) or goat anti-rabbit 488 (A11008), Thermo Fisher Scientific). Cells were then treated with DAPI at a 1:5,000 dilution for 5 minutes, and washed in PBS prior to imaging of 2 biological replicates on a Zeiss Cell Observer Spinning Disk (Carl Zeiss AG).

Matrix Decellularization. Cells were cultured on PEG-PC gels of 1, 4, 8, and 41 kPa for 24 hours or 6 days, and the resulting matrix created by the cells was visualized by adapting a previously published protocol [35]. Briefly, cells were washed with warm PBS, then lysed with 500µL warm extraction buffer (PBS with 0.5% Triton-X with 20 mM ammonium hydroxide) for 10 minutes at room temperature. 1 mL of PBS was added and the gels were stored overnight at 4°C before staining as described above.

Protein and Phospho-protein Quantification. Autolyzed calpain 2 and talin were analyzed via western blot. Cells were cultured on PEG-PC gels of 1 or 41 kPa for 24 hours, then lysed in RIPA buffer with protease inhibitors: 1 cOmplete Mini EDTA-free Protease inhibitor cocktail tablet per 10 mL (Roche, Indianapolis, IN) 1 mM phenylmethylsulfonyl fluoride (Thermo Fisher Scientific), 5 µg mL^{-1} pepstatin A (Thermo Fisher Scientific), 10 µg mL^{-1} of leupeptin (Thermo Fisher Scientific), and phosphatase inhibitors: Phosphatase inhibitors cocktail-II (Boston Bioproducts, Boston, MA), 1 mM sodium pyrophosphate (Thermo Fisher

Scientific), 25 mM β-glycerophosphate (Santa Cruz, Dallas, TX). Lysates were prepared in a 5x reducing sample buffer (39000, Thermo Fisher Scientific), run on Tris-Glycine gels in an Invitrogen mini-Xcell Surelock system, then transferred to nitrocellulose membranes (88018, Life Technologies, CA). Membranes were blocked with Abdil for 1 hour, then stained overnight at 4°C with antibodies against calpain 2 (MABT505, 1:1000, Millipore), integrin α_6 (ab134565, 1:2000, Abcam), EGFR (D38B1, 1:1000, Cell Signaling Technology, Danvers, MA), talin (ab157808, 1:1000, Abcam), GAPDH (ab9485, 1:2000, Abcam) or β-actin (ab75186, 1:1000, Abcam). Membranes were washed 3 times with TBS-T, stained in secondary antibody (Goat anti-rabbit 680 (926-68021, 1:20,000) and Donkey anti-mouse 800 (926-32212, 1:10,000), LiCor, Lincoln, NE) for 1 hour at room temperature, protected from light, and washed 3 times in TBS-T with a final wash in TBS. Membranes were imaged on the Odyssey CLx (Licor). Image J was used to quantify calpain 2 and talin bands.

2 biological replicates of lysates were collected during cell adhesion at 0, 5, 30, and 60 minutes, and 24 hours. At 0, 5, 30, and 60 minutes, the adhered fraction was lysed off the surface, while suspended cells were pelleted, then lysis buffer was added. These 2 fractions were combined for analysis. Phospho-protein levels were quantified with the MAGPIX system (Luminex, Austin, Texas) with MILLIPLEX MAP Multi-Pathway Magnetic Bead 9-Plex - Cell Signaling Multiplex Assay (48-681MAG, Millipore) and added beads against p-EGFR (pan-tyrosine, 46-603MAG, Millipore), p-MEK (Ser222, 46-670MAG, Millipore), and p-ERK1/2 (Thr185/Tyr187, 46-602MAG, Millipore), following the manufacturer's protocols.

Co-Immunoprecipitation. MDA-MB-231 cells were grown to confluence in a T-75 cell culture flask. Cells were treated with 10 mL of fresh media containing 10% FBS, with or without an additional 100 ng mL^{-1} EGF for 10 minutes. Flasks were lysed in 4.5 mL of lysis buffer, comprised of 50 mM Tris (pH 7.4), 0.15 M NaCl, 0.1% Triton-X, with protease and phosphatase inhibitors as described above. 1 mL of lysate was immunoprecipitated with 10 µL agarose beads (Thermo Fisher Scientific) with either 5 µL rabbit IgG (ab6718, Abcam), 10 µL anti-EGFR (D38B1, Cell Signaling), or with 10 µL anti-EGFR pre-conjugated to sepharose beads (5735S, Cell Signaling). Lysates were precipitated on beads overnight at 4°C on a rotating platform and

spun down. Beads (with protein) were washed 3x with TBS, and boiled in 70 µL of DiH_2O and sample buffer. Blotting was done as described above for pEGFR (ab32430, Abcam) and integrin α_6 (ab134565, Abcam).

Statistical Analysis. One-way Analysis of Variance (ANOVA) with a Tukey post-test was performed on paired samples using Prism v5.04 (Graphpad software, La Jolla, CA). Data reported is the mean and reported error is standard deviation with significance values of $p \leq 0.05$ as *, $p \leq 0.01$ as **, and $p \leq 0.001$ as ***.

Results

Cells Maximize Expression of Integrin α_6 and Extracellular Laminin on Soft Substrates

To identify ECM and integrin-associated genes involved in breast cancer mechanosensing, we performed whole transcriptome sequencing (RNA-Seq) on MDA-MB-231 cells cultured on collagen 1-functionalized PEG-PC hydrogels ranging in stiffness from 1 to 41 kPa for either 24 hours or 6 days (Fig. S1). The stiffness range chosen spans that of several tissues in the body where breast cancer metastasizes (1 kPa- brain [36], 4 kPa- bone marrow [37], 8 kPa- lung [38]), as well as a supra-physiological stiffness (41 kPa) that approximates extremely stiff breast tumors [39] and a tissue culture polystyrene (TCPS) control (Fig. S1).

Because the ECM is known to regulate the ability of cancer cells to migrate and metastasize, we focused our in-depth analysis of this RNA-Seq data set on genes that regulate interaction with the ECM. We found that the expression of integrins, other focal adhesion complex genes, and genes downstream of EGFR phosphorylation were sensitive to stiffness (Fig. S1, Fig. 1a-b). Short-term (24 hour) decreases in expression were clear in integrin α_6, calpain 2, and integrin β_4 (Fig. 1a). Integrin β_4 expression was 3-fold higher on gels by day 6 (Fig. 1b). This likely induces a switch in dimer pairs, as integrin α_6 preferentially dimerizes with integrin β_4 over integrin β_1 [40], and is known to regulate cancer cell invasion and motility [41].

Given that integrin $\alpha_6\beta_4$ is laminin-binding and we saw mechanosensitive changes in gene and protein expression (Fig. S2a), we hypothesized that we could tune integrin α_6 mechanosensing on these surfaces by supplementing the collagen-functionalized hydrogel surfaces with β_1-chain-containing laminins. On soft gels, integrin α_6 expression was higher at 24 hours with added laminin compared to collagen 1 only and, interestingly, it was also high after 6 days of culture, even without laminin (Fig. 1c). This mechanosensitivity appears to be specific to α_6 as other laminin-binding integrins (e.g. integrin α_3) did not follow this trend (Fig. S2b).

We hypothesized that cells must be producing their own laminin to initiate integrin α_6 expression at the longer culture times. Immunofluorescent staining revealed that laminin, but not collagen 1, was upregulated on

the softer gels at 6 days (Fig. 1d). We separately confirmed that differential staining was not due to ECM proteins provided to the cells either via covalent crosslinking or from serum (Fig. S3). Cultures that were decellularized after 6 days of culture showed the highest amount of extracellular laminin on the softest, 1 kPa gels (Fig. 1d), concordant with the increase in integrin α_6 expression in Figure 1c.

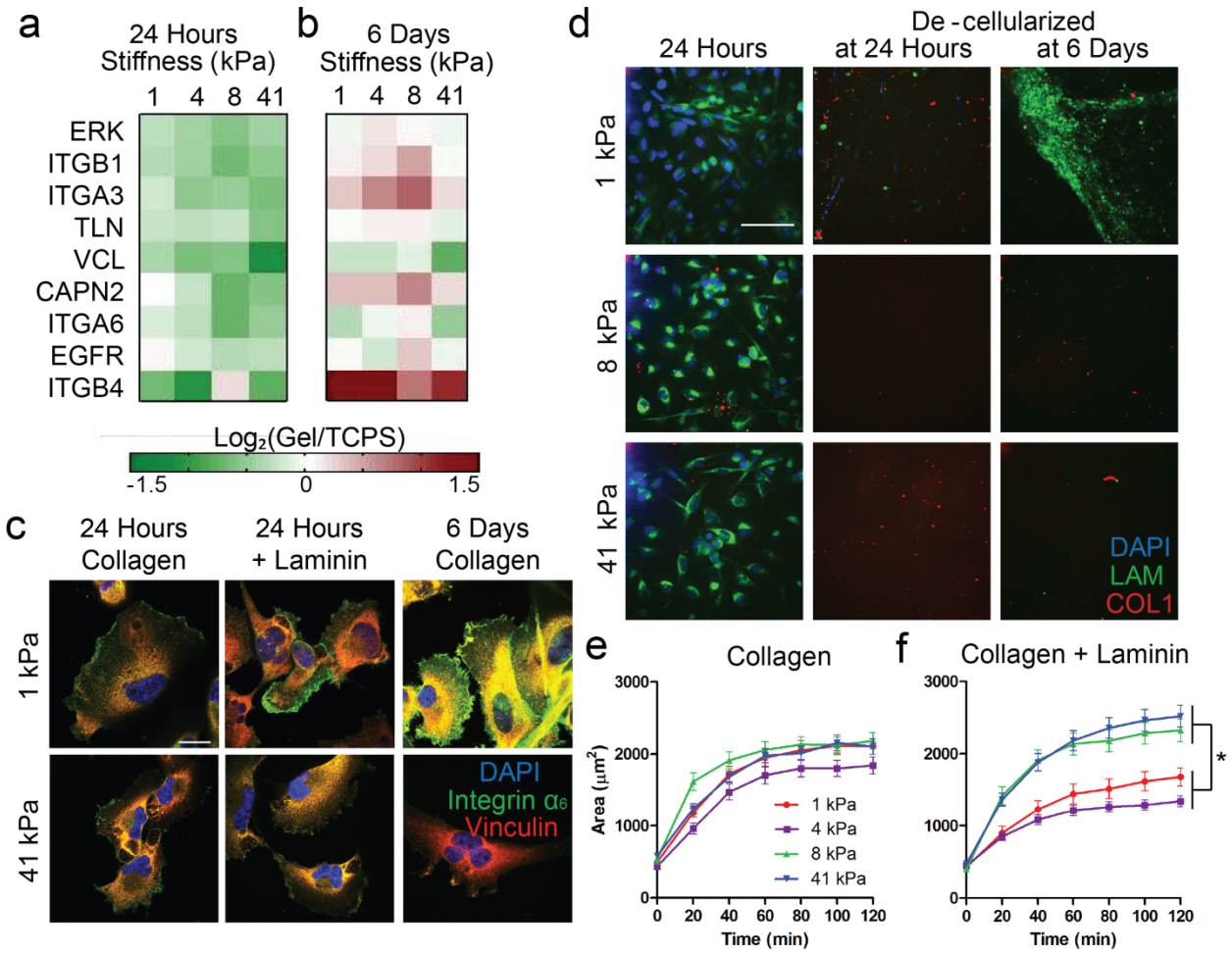

Figure 1. Cells on soft substrates have increased integrin α_6 expression and produce extracellular laminin. (a-b) Log_2(fold change) of gene expression from cells cultured on gels of stiffnesses 1, 4, 8 or 41 kPa relative to expression on TCPS of genes identified from RNA-seq after 24 hours (a) or 6 days (b), determined through qRT-PCR. Decreased expression = green and increased expression = red. (c) Immunofluorescent staining of vinculin (red) and integrin α_6 (green) and DAPI (blue) in cells cultured on gels with collagen only for 24 hours, collagen with laminin for 24 hours, or collagen only for 6 days. Scale bar = 20 μm. (d) Immunofluorescent staining for ECM proteins after 1 day of culture (left), decellularized gels after 24 hours (center) or decellularized gels after 6 days (right). Collagen 1 = red, pan-laminin = green, DAPI = blue. Scale bar = 100 μm. (e-f) Cell area during adhesion quantified on 1, 4, 8, and 41 kPa gels functionalized with collagen 1 only (e) or collagen 1 + laminin (f).

To understand the impact of laminin and integrin α_6 expression on cell adhesion to the gels, we quantified cell spreading during initial adhesion. We found cells spread to similar extents across the 4 stiffnesses examined here when only collagen 1 was present (Fig. 1e). When laminin was added to the collagen on the gel surfaces, cells spread to a smaller extent, on soft, but not stiff gels (Fig. 1f). In sum, cells upregulate integrin α_6 expression on soft substrates, which is correlated with secretion of extracellular laminin. This coordination appears to take several days, but the mechanosensitivity effect on cell spreading can be accelerated by adding β_1-chain-containing laminin to the culture substrata.

Cell Response to EGF Stimulation Mirrors Mechanosensing on Laminin

Given the prevalence of EGF in the tumor microenvironment and its known role in promoting cancer cell motility, we posited that the mechanosensitive expression of EGFR alongside the laminin-binding integrin α_6 could hint that they mechanotransduce under a related pathway. Similar to previous reports, we found that MDA-MB-231 cells were smaller on both 1 and 41 kPa gels upon the addition of EGF prior to and during adhesion [34], achieving a similar size to cells on soft, laminin-coated gels (Fig. 2a). EGFR is known to associate with the $\alpha_6\beta_4$ integrin dimer to enhance clustering and response to EGF [42], and we found that the addition of soluble EGF increased the association of integrin α_6 with EGFR (Fig. S4a). We separately analyzed the protein expression of integrin α_6 and EGFR in tropic variants of the MDA-MB-231 cell line, which were selected *in vivo* for their ability to metastasize specifically to the brain, bone, and lung. We noted that the brain tropic cells, which metastasize to the softest of these sites, have the highest expression of both integrin α_6 and EGFR (Fig. S4b).

To test the necessity of integrin α_6 in the observed response to EGF, we generated a stable shRNA knockdown cell line (Fig. S4c-e). We then quantified adhesion of the integrin α_6 knockdown cells (shITGA6) to collagen-coated gels, and found that they remained large during EGF stimulation, compared to the scramble control (shSCR), suggesting that integrin α_6 is required for the typical EGF response (Fig. 2b).

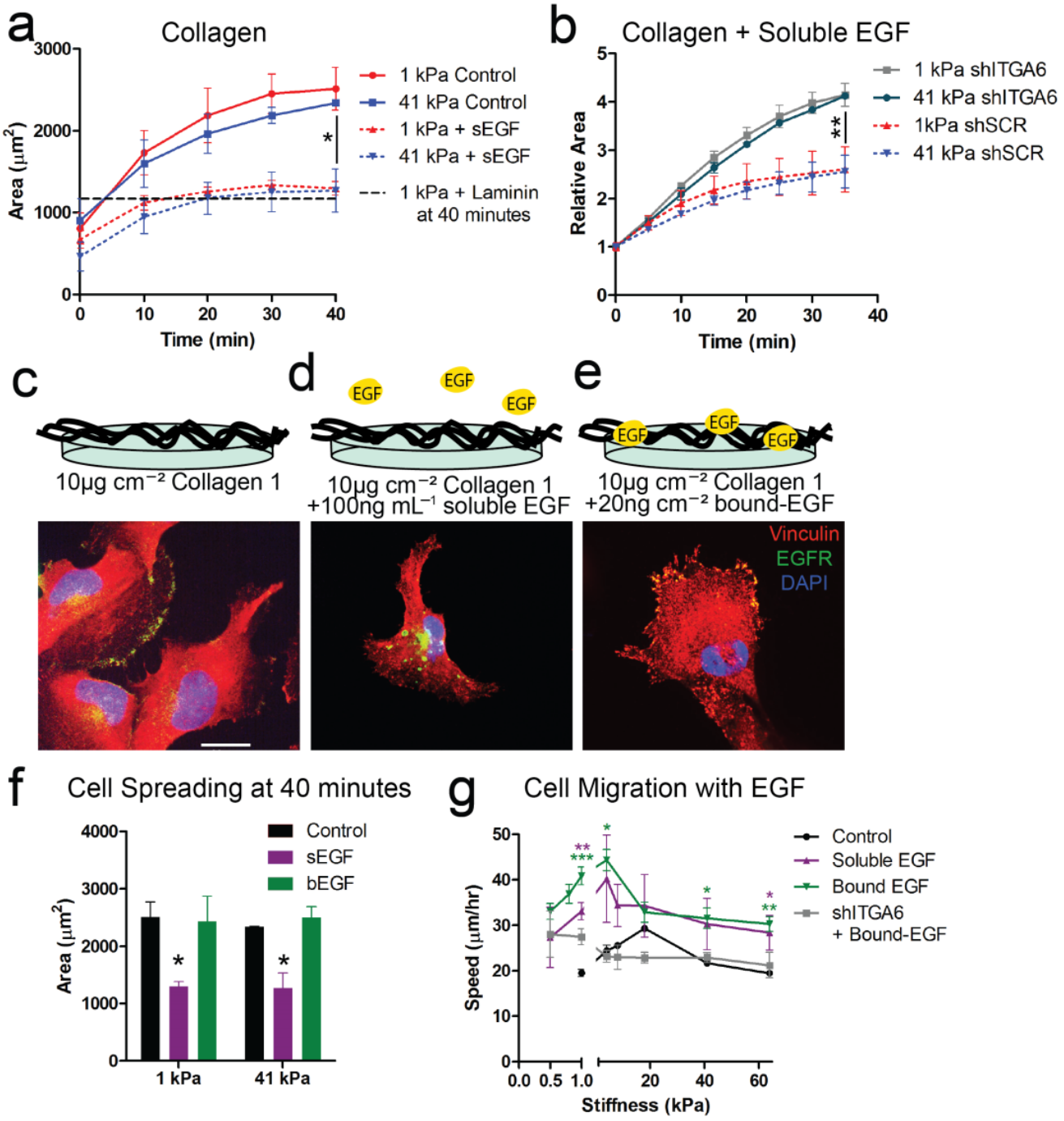

Figure 2. Addition of EGF mimics of the mechanosensitivity effect of soft, laminin containing surfaces. (a) Cell area during adhesion with soluble EGF is compared to data from Fig. 1d-e. (b) Change in area during cell adhesion of integrin α_6 knockdown cells (shITGA6) compared to scramble control cells (shSCR). (c-e) Cells were cultured on collagen with either no EGF (c), 100 ng mL^{-1} soluble EGF for 10 minutes (d), or 20 ng cm^{-2} EGF bound to the surface for 24 hours (e). Scale bar = 20 μm. Fixed cells were stained for vinculin (red), total EGFR (green), and DAPI (blue). (f) Area was quantified 40 minutes after adhesion to 10 μg cm^{-2} collagen 1 with no EGF, soluble EGF (sEGF), or bound EGF (bEGF). (g) Parental MDA-MB-231 cell speeds were quantified on 10 μg cm^{-2} collagen 1 with no EGF, with 10 ng mL^{-1} soluble EGF, 20 ng cm^{-2} bound EGF. shITGA6 cell speeds were quantified on 10 μg cm^{-2} collagen 1 + 20 ng cm^{-2} bound EGF.

Substrate-Bound EGF Restrains EGFR to Focal Adhesions and Maximizes Cell Motility on Soft Substrates

EGF in solution is rapidly internalized within 10 minutes of administration *in vitro* (Fig. 2c-d). To maximize the likelihood of sustained interactions between EGFR and integrin α_6 necessary for downstream signaling [42], we covalently linked both collagen 1 and EGF to the surface of the PEG-PC gels (Fig. 2e). This EGF presentation minimized EGFR internalization (Fig. 2e) and localized both pEGFR(Y1068) and total EGFR to regions of vinculin staining (Fig. S5a-b), suggesting this surface bound EGF facilitates cooperative signaling between integrins and EGFR.

EGFR receptor internalization was required to alter adhesion, as only cells seeded with soluble EGF showed measurable differences in cell area (Fig. 2f). However, both bound and soluble EGF had large effects on cell motility. First, we observed a biphasic trend in cell speed with respect to stiffness, as previously described [7]. The addition of soluble or bound EGF increased overall motility on both soft and stiff substrates (Fig. 2g). In fact, we were forced to expand the mechanical range of the hydrogels to much softer conditions to capture the full biphasic curve during EGF stimulation (Fig. S5c) [26]. We also observed a role for integrin α_6 in regulating this EGF-dependent motility, as the integrin α_6 knockdown population (shITGA6) was significantly less responsive to EGF than the scramble control cells, which peaked at 34.2 μm/hr on 1 kPa gels (Fig. 2g, grey line, Fig. S5d).

Calpain 2 is Downstream of EGFR and Integrin α_6 Mechanosensing

Inspired by the RNAseq data (Fig. S1), we wondered whether calpain 2 was an intracellular protein downstream of both EGFR and integrin α_6 mechanosensitivity. PCR data at 24 hours of culture on different substrates uncovered that *ITGA6* and *EGFR* expression clustered with the intracellular protease *CAPN2* (Fig. 3a). Calpain 2, which has been implicated in focal adhesion formation and disassembly, is thought to play an important role in breast cancer cell motility and metastasis [43]. Because calpain 2 is activated by ERK [44], we performed phospho-analysis of multiple kinases in integrin- and EGFR-dependent pathways (Fig. S6a). Only

MEK and ERK were phosphorylated significantly above background in our system on 1 kPa, 41 kPa and TCPS (Fig. S6b). Steady-state phosphorylation of EGFR, MEK, and ERK increased on stiffer surfaces, as previously demonstrated [17, 45, 46]. However, we observed the opposite trend with the activation of calpain 2, and the cleavage of its substrate, talin (Fig. S6c).

We observed more sustained calpain 2 activity (autolysis) during adhesion to hydrogels compared to tissue culture plastic (Fig. 3b). This was only a slight trend; however, there was an obvious functional role for calpain 2 during mechanosensing on the gels. A pharmacological inhibitor to either calpain 2 or ERK had no effect on cell spreading on 1 kPa gels, but resulted in significantly larger cells on 41 kPa gels (Fig. 3c-d). To confirm the necessity of calpain 2 in responding to EGF stimulation, we generated a *CAPN2* knockdown cell line (Fig. S7a-c), and observed that those cells were less responsive to EGF during adhesion, independent of stiffness (Fig. S7d).

We further hypothesized that calpain 2 could disturb the typical biphasic relationship between cell migration speed and matrix stiffness given its known role in mediating focal adhesion turnover [44]. Inhibiting ERK activity entirely eliminated the durokinesis effect, and calpain 2 inhibition shifted the migration curve maximum to lower stiffnesses (Fig. 3e). The limiting step during motility on stiff surfaces is retraction of the rear edge [47]. Here we demonstrate that motility on stiff substrates is sensitive to calpain 2 inhibition, likely because cells on stiffer surfaces have decreased basal calpain 2 activity (Fig. S6c). After 24 hours of culture on PEG-PC gels with collagen 1 or collagen 1 and bound EGF, cells adopted a normal morphology with no noticeable protrusions (Fig. 3f). However, in the presence of lapatinib (dual kinase EGFR-HER2 inhibitor), ERK inhibitor, or calpain 2 inhibitor, we observed that cells left behind long, stable protrusions at the rear of the cell, indicative of their inability to release adhesion sites (Fig. 3g) [48]. While we demonstrated earlier that integrin α_6 is necessary for both mechanosensitive and EGFR-mediated adhesion, this data suggests that EGFR-ERK-calpain 2 signaling contributes to mechanosensitive motility necessary for breast cancer metastasis.

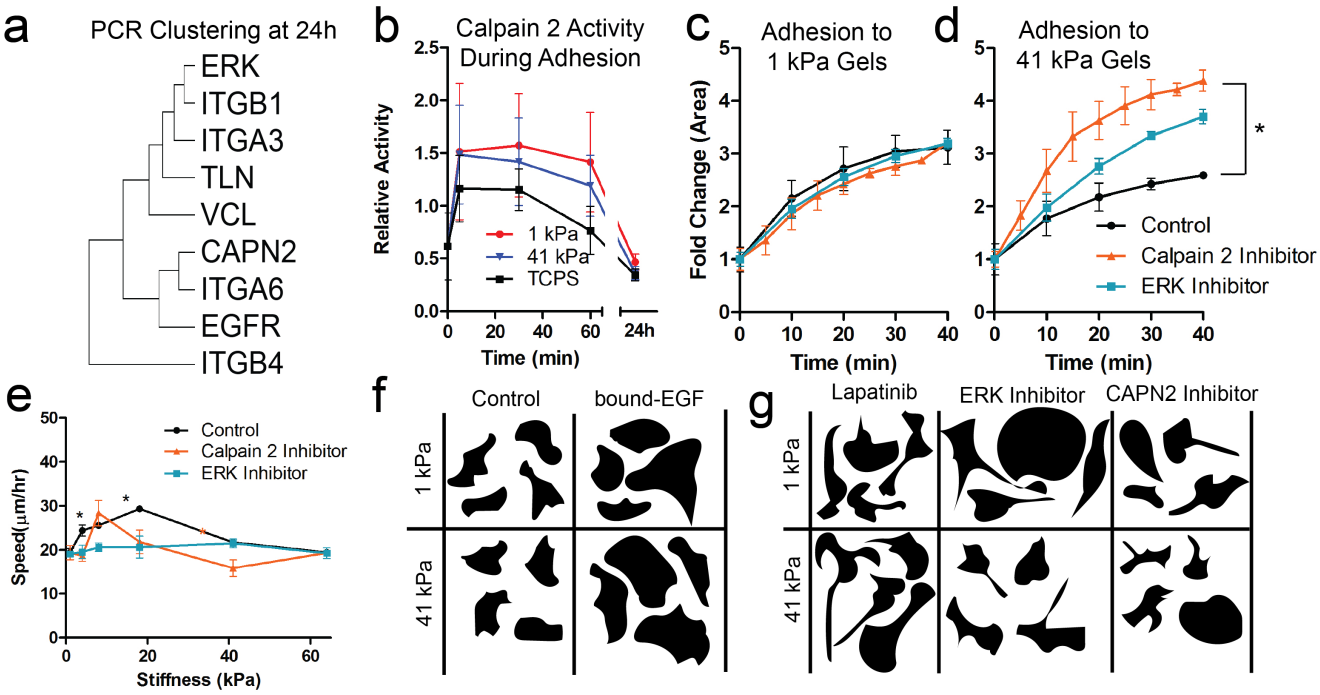

Figure 3. Calpain 2 is downstream of both mechanosensitive integrin α_6 and EGFR. (a) Clustering of PCR data on genes expressed after 24 hours of culture on gels functionalized with 10μg/cm^2 collagen 1 (data in Fig. 1a). (b) Calpain 2 activity during adhesion was measured by evaluating the ratio of autolyzed/full length calpain 2 via western blot in both the adhered and suspended cell fractions during the first 60 minutes, or just the adhered fraction after 24 hours. (c-d) Cell area was quantified during adhesion in the presence of an ERK1/2 inhibitor or calpain 2 inhibitor on 1 kPa (c) and 41 kPa (d) gels. (e) Cell migration speeds quantified the presence of an ERK1/2 or calpain 2 inhibitor. (f) Cell morphology was analyzed 24 hours after seeding onto PEG-PC gels of 1 or 41 kPa functionalized with either 10ug cm^{-2} collagen 1 or 10ug cm^{-2} collagen 1+ 20 ng cm^{-2} EGF. (g) Cells were dosed with lapatinib, ERK inhibitor, or calpain 2 inhibitor 22 hours after seeding onto PEG-PC gels of 1 or 41 kPa. Cell morphology was analyzed 2 hours after treatment with inhibitors.

Discussion

This work demonstrates integrin α_6 and calpain 2 as mechanosensitive proteins important for stiffness-driven breast cancer cell adhesion and migration (Fig. 4a). The mechanosensitivity of calpain 2 is a new finding, as well as the required physical association of EGFR with integrin α_6 to facilitate cell adhesion (Fig. 4b). EGF is known to enhance breast cancer cell adhesion and motility, and here we demonstrate that the mechanosensitive integrin α_6-calpain 2 signaling axis can mimic the effect of EGF-stimulated cell adhesion and motility (Fig. 4c).

Cancer metastasis initiates with individual or collective groups of cells leaving the primary tumor site [49-51]. This motility is driven in part by cell-ECM adhesion via integrins and the creation and turnover of focal adhesions, both of which are known to be sensitive to the stiffness of the surrounding ECM [52]. Integrins have variable responses to mechanical forces derived from the microenvironment. For example, on 2D gels, integrin β_3 stiffness-dependence requires surface bound BMP-2 [21]. Expression of integrins α_2, α_3, and β_1 are higher on TCPS in mouse mammary epithelial cells, when compared to plating on a soft basement membrane-like matrix [53]. Integrin α_5 expression was also found to increase 5-fold with stiffness between 1 kPa and 10 kPa [54]. While most previous work has focused on the mechanical regulation of collagen- and fibronectin-binding integrins, one group has examined integrin α_6 in fibroblasts, where expression increases with stiffness to cause an increase in invasion [55]. We demonstrate here the integrin α_6 expression response in breast cancer cells, and its mechanosensitivity in cell adhesion, migration, and response to EGF (Fig. 1c, Fig. 2b). Integrin α_6 is a laminin-binding subunit, and so translating its mechanosensitive expression to altered mechanotransduction requires the addition of laminin to the culture substrate. On soft surfaces, cells produce extracellular laminin to engage integrin α_6 in the absence of exogenously provided ligand.

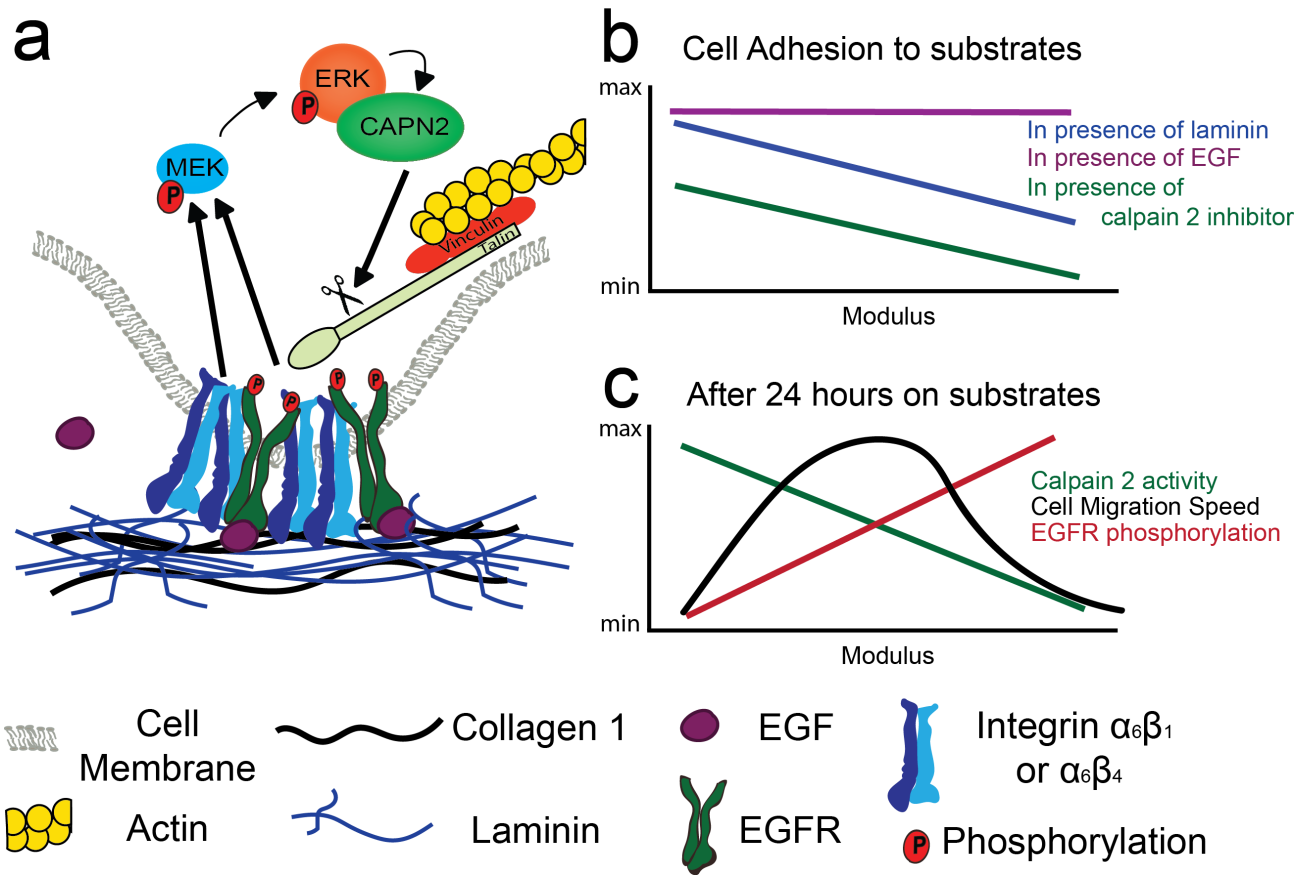

Figure 4. Mechanosensitive signaling is dependent on laminin and substrate stiffness. (a) Breast cancer cells on soft gels, or any stiffness gel supplemented with EGF, were small and motile. Cells on soft gels produced their own laminin to engage α_6, or we added it exogenously. Our data suggests this increases activation of ERK and Calpain 2, which feeds back to increase turnover of focal adhesions. (b) During adhesion to substrates, cells were more responsive to laminin on soft substrates but did not adhere as well on stiff substrates with a calpain 2 inhibitor. Cell adhesion was facilitated in the presence of EGF on both soft and stiff gels. (c) After 24 hours on gels, calpain 2 activity decreased with increasing stiffness, while EGFR phosphorylation increased with stiffness without added EGF. Cell motility had a biphasic dependence on substrate stiffness.

Previous work has established the role of integrin α_6 in key aspects of the metastatic cascade. Low integrin α_6 expression inhibits the migration and proliferation necessary for establishing metastases at distant secondary sites [56]. Additionally, integrin α_6 expression can protect cells from radiotherapy treatment both through PI3K and MAPK activity [57]. We observed that during cell adhesion, integrin α_6 engagement with laminin decreases cell size and facilitates adhesion similarly to EGF (Fig. 2a-b). Smaller cells can be correlated with a cancer stem cell and invasive phenotype [58], and our work suggests integrin-mediated mechanotransduction contributes to that behavior. Our breast cancer cells produce laminin intracellularly within the first 24 hours and this laminin is

secreted by 6 days of culture with the most laminin produced on the softest substrate (Fig. 1d). Interestingly, this phenomenon is not maintained in other secreted ECM proteins, such as collagen 1 (Fig. 1d) or fibronectin (data not shown), suggesting a key role for integrin α_6-mediated adhesion to laminin on soft surfaces. This is possibly mediated through the mechanically responsive transcription factor, TAZ [59], which has been shown to regulate laminin production [60].

In a cohort of 80 patients, integrin β_4 was co-expressed with integrin α_6 and laminin in primary tumors, and that co-expression of $\alpha_6\beta_4$ with laminin production was significantly correlated with breast cancer relapse and death [40, 61]. We found that both integrin β_4 expression and laminin production were enhanced after 6 days of culture on soft gels (Fig. 1b, Fig. 1d), indicating these cells have adopted a more aggressive phenotype. Downstream of integrin α_6 engagement and EGFR phosphorylation, cells activate calpain 2, which facilitates focal adhesion turnover, and therefore, motility (Fig. 3e). Recent work has also demonstrated that calpains are recruited to protrusions containing integrin β_4 [62]. The $\alpha_6\beta_4$ integrin dimer associates with EGFR, which enhances receptor clustering and increases cellular capacity to respond to EGF (Fig. 2b) [42]. Here, we contribute that in breast cancer cells, integrin α_6 shows increased expression on the softest substrates, where adhesion to laminin mimics the phenotype induced by EGF. This provides insight to the effect of mechanics on adhesion formation in the tumor microenvironment.

Previous work has shown that EGF enhances cell speed while decreasing persistence [63], and here we demonstrate that during migration the effect of EGF on migration speed is significant on soft and stiff, but not intermediate substrates, where speed is already maximized (Fig. 2g). Motility is preferentially driven by surface localized EGFR, and we demonstrate that bound EGF restrains EGFR at the cell membrane (Fig. 2e) to enhance phosphorylation of Y1068 on EGFR (Fig S5a). Triggered by either ligand binding or integrin clustering, EGFR activates ERK [64] and subsequent ERK activity is localized to newly formed focal adhesions to propagate a local downstream response [65, 66].

Localized EGFR phosphorylation is necessary for activity in downstream effectors, including MEK, ERK, and calpain 2 at the cell membrane [67, 68], to cleave focal adhesion proteins vinculin, talin, paxillin, and FAK

[69, 70]. During adhesion, calpain 2 activity was sustained on the hydrogels compared to TCPS, which was consistent with RNA levels and steady state cleavage of calpain 2 and talin (Fig. 1a-b, Fig. S6c). Calpain 2 inhibition during adhesion resulted in larger, less motile cells, particularly on stiff substrates. Cells were smaller at both 1 and 41 kPa in the presence of soluble EGF (Fig. 2a). Together, these data suggest that EGFR phosphorylation could be a stronger activator of calpain 2 than stiffness. Previous work has shown that calpain 2 has a significant correlation with an epithelial-to-mesenchymal transition [71] and lymphatic or vascular invasion, where patients with basal-like tumors and high calpain 2 expression had a significantly worse prognosis [72]. Our work demonstrates a mechanosensitive role for calpain 2, providing further evidence for its potential as a druggable target for metastatic breast cancer. In sum, both integrin α_6 and EGF regulate cell motility, and these pathways converge at stiffness-dependent calpain 2 activity.

Conclusions

Mechanical forces have long been thought to play a role in tumor progression, and here we shed light on two mechanoresponsive proteins that influence breast cancer cell motility. First, enhanced integrin α_6 expression on soft substrates is associated with adhesion on a basement membrane-like environment and laminin production. Second, clustering and cooperative signaling between EGFR and focal adhesion proteins, such as integrin α_6, increases activity of calpain 2 on soft substrates, which mediates the destabilization and turnover of focal adhesions necessary for motility. Others have suggested targeting calpains to inhibit cancer cell invasion [73], and here we provide a mechanistic understanding of the role of calpain 2 in stiffer environments that may better recapitulate the tumor microenvironment.

Author Contributions

ADS, SRP, and CCB participated in experimental design. ADS, CLH, and LEB performed experiments. All authors discussed results and contributed to editing of the manuscript.

Conflict of Interest

The authors declare no conflict of interest.

Data Availability

RNAseq data is available under GEO accession number GSE92653.

Acknowledgements

This work was supported by a National Science Foundation Graduate Research Fellowship to ADS (Award 1451512), a National Institutes of Health grant to SRP (1DP2CA186573-01), a CAREER grant from the NSF to SRP (DMR-153514) and the University of Massachusetts, Amherst. SRP is a Pew Biomedical Scholar supported by the Pew Charitable Trusts and a Barry and Afsaneh Siadat faculty award. LEB was partially supported by National Research Service Award T32 GM008515 from the National Institutes of Health.

References

1. Kraning-Rush, C.M., J.P. Califano, and C.A. Reinhart-King, *Cellular traction stresses increase with increasing metastatic potential.* PLoS One, 2012. **7**(2): p. e32572.
2. Chandler, E.M., B.R. Seo, J.P. Califano, R.C. Andresen Eguiluz, J.S. Lee, C.J. Yoon, D.T. Tims, J.X. Wang, L. Cheng, S. Mohanan, M.R. Buckley, I. Cohen, A.Y. Nikitin, R.M. Williams, D. Gourdon, C.A. Reinhart-King, and C. Fischbach, *Implanted adipose progenitor cells as physicochemical regulators of breast cancer.* Proc Natl Acad Sci U S A, 2012. **109**(25): p. 9786-91.
3. Cox, T.R. and J.T. Erler, *Remodeling and homeostasis of the extracellular matrix: implications for fibrotic diseases and cancer.* Dis Model Mech, 2011. **4**(2): p. 165-78.
4. Wong, S.Y., T.A. Ulrich, L.P. Deleyrolle, J.L. MacKay, J.M. Lin, R.T. Martuscello, M.A. Jundi, B.A. Reynolds, and S. Kumar, *Constitutive activation of myosin-dependent contractility sensitizes glioma tumor-initiating cells to mechanical inputs and reduces tissue invasion.* Cancer Res, 2015. **75**(6): p. 1113-22.
5. Wen, J.H., O. Choi, H. Taylor-Weiner, A. Fuhrmann, J.V. Karpiak, A. Almutairi, and A.J. Engler, *Haptotaxis is cell type specific and limited by substrate adhesiveness.* Cell Mol Bioeng, 2015. **8**(4): p. 530-542.
6. Wang, L., B. Sun, K.S. Ziemer, G.A. Barabino, and R.L. Carrier, *Chemical and physical modifications to poly(dimethylsiloxane) surfaces affect adhesion of Caco-2 cells.* J Biomed Mater Res A, 2010. **93**(4): p. 1260-71.
7. Peyton, S.R. and A.J. Putnam, *Extracellular matrix rigidity governs smooth muscle cell motility in a biphasic fashion.* J Cell Physiol, 2005. **204**(1): p. 198-209.
8. Seo, B.R., P. Bhardwaj, S. Choi, J. Gonzalez, R.C.A. Eguiluz, K. Wang, S. Mohanan, P.G. Morris, B. Du, X.K. Zhou, L.T. Vahdat, A. Verma, O. Elemento, C.A. Hudis, R.M. Williams, D. Gourdon, A.J. Dannenberg, and C. Fischbach, *Obesity-dependent changes in interstitial ECM mechanics promote breast tumorigenesis.* Sci Trans Med, 2015. **7**(301).
9. Booth-Gauthier, E.A., T.A. Alcoser, G. Yang, and K.N. Dahl, *Force-induced changes in subnuclear movement and rheology.* Biophys J, 2012. **103**(12): p. 2423-31.
10. Provenzano, I., Eliceiri, Keely, *Matrix density-induced mechanoregulation of breast cell phenotype, signaling and gene expression through a FAK–ERK linkage.* Oncogene, 2009. **28**: p. 4326–4343.
11. Yao, M., B.T. Goult, B. Klapholz, X. Hu, C.P. Toseland, Y. Guo, P. Cong, M.P. Sheetz, and J. Yan, *The mechanical response of talin.* Nat Commun, 2016. **7**: p. 11966.
12. Kumar, A., M. Ouyang, K. Van den Dries, E.J. McGhee, K. Tanaka, M.D. Anderson, A. Groisman, B.T. Goult, K.I. Anderson, and M.A. Schwartz, *Talin tension sensor reveals novel features of focal adhesion force transmission and mechanosensitivity.* J Cell Biol, 2016. **213**(3): p. 371-83.
13. Levental, K.R., H. Yu, L. Kass, J.N. Lakins, M. Egeblad, J.T. Erler, S.F. Fong, K. Csiszar, A. Giaccia, W. Weninger, M. Yamauchi, D.L. Gasser, and V.M. Weaver, *Matrix crosslinking forces tumor progression by enhancing integrin signaling.* Cell, 2009. **139**(5): p. 891-906.
14. Bischofs, I.B. and U.S. Schwarz, *Cell organization in soft media due to active mechanosensing.* Proc Natl Acad Sci U S A, 2003. **100**(16): p. 9274-9.
15. Alcaraz, J., R. Xu, H. Mori, C.M. Nelson, R. Mroue, V.A. Spencer, D. Brownfield, D.C. Radisky, C. Bustamante, and M.J. Bissell, *Laminin and biomimetic extracellular*

elasticity enhance functional differentiation in mammary epithelia. EMBO J, 2008. **27**: p. 2829-2838.

16. Zhang, X., M.V. Fournier, J.L. Ware, M.J. Bissell, A. Yacoub, and Z.E. Zehner, *Inhibition of vimentin or beta1 integrin reverts morphology of prostate tumor cells grown in laminin-rich extracellular matrix gels and reduces tumor growth in vivo.* Mol Cancer Ther, 2009. **8**(3): p. 499-508.
17. Umesh, V., A.D. Rape, T.A. Ulrich, and S. Kumar, *Microenvironmental stiffness enhances glioma cell proliferation by stimulating epidermal growth factor receptor signaling.* PLoS One, 2014. **9**(7): p. e101771.
18. Saxena, M., S. Liu, B. Yang, C. Hajal, R. Changede, J. Hu, H. Wolfenson, J. Hone, and M.P. Sheetz, *EGFR and HER2 activate rigidity sensing only on rigid matrices.* Nat Mater, 2017.
19. Murphy, L.C., L.J. Murphy, D. Dubik, G.I. Bell, and R.P.C. Shiu, *Epidermal Growth Factor Gene Expression in Human Breast Cancer Cells: Regulation of Expression by Progestins.* Cancer Res, 1988. **48**: p. 4555-4560.
20. Stuhlmiller, T.J., S.M. Miller, J.S. Zawistowski, K. Nakamura, A.S. Beltran, J.S. Duncan, S.P. Angus, K.A. Collins, D.A. Granger, R.A. Reuther, L.M. Graves, S.M. Gomez, P.F. Kuan, J.S. Parker, X. Chen, N. Sciaky, L.A. Carey, H.S. Earp, J. Jin, and G.L. Johnson, *Inhibition of Lapatinib-Induced Kinome Reprogramming in ERBB2-Positive Breast Cancer by Targeting BET Family Bromodomains.* Cell Rep, 2015. **11**(3): p. 390-404.
21. Fourel, L., A. Valat, E. Faurobert, R. Guillot, I. Bourrin-Reynard, K. Ren, L. Lafanechere, E. Planus, C. Picart, and C. Albiges-Rizo, *beta3 integrin-mediated spreading induced by matrix-bound BMP-2 controls Smad signaling in a stiffness-independent manner.* J Cell Biol, 2016. **212**(6): p. 693-706.
22. Moro, L., L. Dolce, S. Cabodi, E. Bergatto, E. Boeri Erba, M. Smeriglio, E. Turco, S.F. Retta, M.G. Giuffrida, M. Venturino, J. Godovac-Zimmermann, A. Conti, E. Schaefer, L. Beguinot, C. Tacchetti, P. Gaggini, L. Silengo, G. Tarone, and P. Defilippi, *Integrin-induced epidermal growth factor (EGF) receptor activation requires c-Src and p130Cas and leads to phosphorylation of specific EGF receptor tyrosines.* J Biol Chem, 2002. **277**(11): p. 9405-14.
23. Kang, Y., P.M. Siegel, W. Shu, M. Drobnjak, S.M. Kakonen, C. Cordón-Cardo, T.A. Guise, and J. Massagué, *A multigenic program mediating breast cancer metastasis to bone.* Cancer Cell, 2003. **3**(6): p. 537-549.
24. Bos, P.D., X.H. Zhang, C. Nadal, W. Shu, R.R. Gomis, D.X. Nguyen, A.J. Minn, M.J. van de Vijver, W.L. Gerald, J.A. Foekens, and J. Massague, *Genes that mediate breast cancer metastasis to the brain.* Nature, 2009. **459**(7249): p. 1005-9.
25. Minn, A.J., G.P. Gupta, P.M. Siegel, P.D. Bos, W. Shu, D.D. Giri, A. Viale, A.B. Olshen, W.L. Gerald, and J. Massague, *Genes that mediate breast cancer metastasis to lung.* Nature, 2005. **436**(7050): p. 518-24.
26. Herrick, W.G., T.V. Nguyen, M. Sleiman, S. McRae, T.S. Emrick, and S.R. Peyton, *PEG-phosphorylcholine hydrogels as tunable and versatile platforms for mechanobiology.* Biomacromolecules, 2013. **14**(7): p. 2294-304.
27. Kim, D., G. Pertea, C. Trapnell, H. Pimentel, R. Kelley, and S.L. Salzberg, *TopHat2: accurate alignment of transcriptomes in the presence of insertions, deletions and gene fusions.* Genome Biol, 2013. **14**.
28. Trapnell, C., L. Pachter, and S.L. Salzberg, *TopHat: discovering splice junctions with RNA-Seq.* Bioinformatics, 2009. **25**(9): p. 1105-11.
29. Trapnell, C., A. Roberts, L. Goff, G. Pertea, D. Kim, D.R. Kelley, H. Pimentel, S.L. Salzberg, J.L. Rinn, and L. Pachter, *Differential gene and transcript expression analysis of RNA-seq experiments with TopHat and Cufflinks.* Nat Protoc, 2012. **7**(3): p. 562-78.

30. Langmead, B., C. Trapnell, M. Pop, and S.L. Salzberg, *Ultrafast and memory-efficient alignment of short DNA sequences to the human genome.* Genome Biol, 2009. **10**(3): p. R25.
31. Roberts, A., C. Trapnell, J. Donaghey, J.L. Rinn, and L. Pachter, *Improving RNA-Seq expression estimates by correcting for fragment bias.* Genome Biol, 2011. **12**.
32. Trapnell, C., B.A. Williams, G. Pertea, A. Mortazavi, G. Kwan, M.J. van Baren, S.L. Salzberg, B.J. Wold, and L. Pachter, *Transcript assembly and quantification by RNA-Seq reveals unannotated transcripts and isoform switching during cell differentiation.* Nat Biotechnol, 2010. **28**(5): p. 511-5.
33. Trapnell, C., D.G. Hendrickson, M. Sauvageau, L. Goff, J.L. Rinn, and L. Pachter, *Differential analysis of gene regulation at transcript resolution with RNA-seq.* Nat Biotechnol, 2013. **31**(1): p. 46-53.
34. Barney, L.E., E.C. Dandley, L.E. Jansen, N.G. Reich, A.M. Mercurio, and S.R. Peyton, *A cell-ECM screening method to predict breast cancer metastasis.* Integr Biol (Camb), 2015. **7**(2): p. 198-212.
35. Castello-Cros, R. and E. Cukierman, *Stromagenesis during tumorigenesis: characterization of tumor-associated fibroblasts and stroma-derived 3D matrices.* Methods Mol Biol, 2009. **522**: p. 275-305.
36. Budday, S., R. Nay, R. de Rooij, P. Steinmann, T. Wyrobek, T.C. Ovaert, and E. Kuhl, *Mechanical properties of gray and white matter brain tissue by indentation.* J Mech Behav Biomed Mater, 2015. **46**: p. 318-30.
37. Jansen, L.E., N.P. Birch, J.D. Schiffman, A.J. Crosby, and S.R. Peyton, *Mechanics of intact bone marrow.* J Mech Behav Biomed Mater, 2015. **50**: p. 299-307.
38. Luque, T., E. Melo, E. Garreta, J. Cortiella, J. Nichols, R. Farre, and D. Navajas, *Local micromechanical properties of decellularized lung scaffolds measured with atomic force microscopy.* Acta Biomater, 2013. **9**(6): p. 6852-9.
39. Samani, A., J. Zubovits, and D. Plewes, *Elastic moduli of normal and pathological human breast tissues: an inversion-technique-based investigation of 169 samples.* Phys Med Biol, 2007. **52**(6): p. 1565-76.
40. Ramovs, V., L. Te Molder, and A. Sonnenberg, *The opposing roles of laminin-binding integrins in cancer.* Matrix Biol, 2016.
41. Shaw, L.M., I. Rabinowitz, H.H.-F. Wang, A. Toker, and A.M. Mercurio, *Activation of Phosphoinositide 3-OH Kinase by the a6B4 Integrin Promotes Carcinoma Invasion.* Cell, 1997. **91**: p. 949-960.
42. Gilcrease, M.Z., X. Zhou, X. Lu, W.A. Woodward, B.E. Hall, and P.J. Morrissey, *Alpha6beta4 integrin crosslinking induces EGFR clustering and promotes EGF-mediated Rho activation in breast cancer.* J Exp Clin Cancer Res, 2009. **28**: p. 67.
43. Franco, S.J. and A. Huttenlocher, *Regulating cell migration: calpains make the cut.* Journal of Cell Science, 2005.
44. Glading, A., P. Chang, D.A. Lauffenburger, and A. Wells, *Epidermal Growth Factor Receptor Activation of Calpain Is Required for Fibroblast Motility and Occurs via an ERK/MAP Kinase Signaling Pathway.* J Biol Chem, 1999. **275**(4): p. 2390-2398.
45. Asthagiri, A.R., C.M. Nelson, A.F. Horowitz, and D.A. Lauffenburger, *Quantitative Relationship among Integrin-Ligand Binding, Adhesion, and Signaling via Focal Adhesion Kinase and Extracellular Signal-regulated Kinase 2.* J Biol Chem, 1999. **274**(38): p. 27119-27127.
46. Hwang, J.H., M.R. Byun, A.R. Kim, K.M. Kim, H.J. Cho, Y.H. Lee, J. Kim, M.G. Jeong, E.S. Hwang, and J.H. Hong, *Extracellular Matrix Stiffness Regulates Osteogenic Differentiation through MAPK Activation.* PLoS One, 2015. **10**(8): p. e0135519.
47. Burnette, D.T., L. Shao, C. Ott, A.M. Pasapera, R.S. Fischer, M.A. Baird, C. Der Loughian, H. Delanoe-Ayari, M.J. Paszek, M.W. Davidson, E. Betzig, and J. Lippincott-

Schwartz, *A contractile and counterbalancing adhesion system controls the 3D shape of crawling cells.* J Cell Biol, 2014. **205**(1): p. 83-96.

48. Palecek, S.P., A. Huttenlocher, A.F. Horwitz, and D.A. Lauffenburger, *Physical and biochemical regulation of integrin release during rear detachment of migrating cells.* JCS, 1998: p. 929-940.
49. Nguyen-Ngoc, K.V., K.J. Cheung, A. Brenot, E.R. Shamir, R.S. Gray, W.C. Hines, P. Yaswen, Z. Werb, and A.J. Ewald, *ECM microenvironment regulates collective migration and local dissemination in normal and malignant mammary epithelium.* Proc Natl Acad Sci U S A, 2012. **109**(39): p. E2595-604.
50. Dasgupta, A., A.R. Lim, and C.M. Ghajar, *Circulating and disseminated tumor cells: Harbiners or metastasis initiators.* Molecular Oncology, 2016.
51. Lee, P. and C.W. Wolgemuth, *Physical Mechanisms of Cancer in the Transition to Metastasis.* Biophys J, 2016. **111**(1): p. 256-66.
52. Weinberg, S.H., D.B. Mair, and C.A. Lemmon, *Mechanotransduction Dynamics at the Cell-Matrix Interface.* Biophys J, 2017. **112**(9): p. 1962-1974.
53. Delcommenne, M. and C.H. Streuli, *Control of Integrin Expression by Extracellular Matrix.* J Biol Chem, 1995. **270**(45): p. 26794-26801.
54. Yeung, T., P.C. Georges, L.A. Flanagan, B. Marg, M. Ortiz, M. Funaki, N. Zahir, W. Ming, V. Weaver, and P.A. Janmey, *Effects of substrate stiffness on cell morphology, cytoskeletal structure, and adhesion.* Cell Motil Cytoskeleton, 2005. **60**(1): p. 24-34.
55. Chen, H., J. Qu, X. Huang, A. Kurundkar, L. Zhu, N. Yang, A. Venado, Q. Ding, G. Liu, V.B. Antony, V.J. Thannickal, and Y. Zhou, *Mechanosensing by the alpha6-integrin confers an invasive fibroblast phenotype and mediates lung fibrosis.* Nat Commun, 2016. **7**: p. 12564.
56. Wang, Y., S. Shenouda, S. Baranwal, R. Rathinam, P. Jain, Lili Bao, S. Hazari, S. Dash, and S.K. Alahari, *Integrin subunits alpha5 and alpha6 regulate cell cycle by modulating the chk1 and Rb/E2F pathways to affect breast cancer metastasis.* Molecular Cancer, 2011.
57. Hu, T., R. Zhou, Y. Zhao, and G. Wu, *Integrin alpha6/Akt/Erk signaling is essential for human breast cancer resistance to radiotherapy.* Sci Rep, 2016. **6**: p. 33376.
58. Ray, A., Z.M. Slama, R.K. Morford, S.A. Madden, and P.P. Provenzano, *Enhanced Directional Migration of Cancer Stem Cells in 3D Aligned Collagen Matrices.* Biophys J, 2017. **112**(5): p. 1023-1036.
59. Dupont, S., L. Morsut, M. Aragona, E. Enzo, S. Giulitti, M. Cordenonsi, F. Zanconato, J. Le Digabel, M. Forcato, S. Bicciato, N. Elvassore, and S. Piccolo, *Role of YAP/TAZ in mechanotransduction.* Nature, 2011. **474**(7350): p. 179-83.
60. Chang, C., H.L. Goel, H. Gao, B. Pursell, L.D. Shultz, D.L. Greiner, S. Ingerpuu, M. Patarroyo, S. Cao, E. Lim, J. Mao, K.K. McKee, P.D. Yurchenco, and A.M. Mercurio, *A laminin 511 matrix is regulated by TAZ and functions as the ligand for the alpha6Bbeta1 integrin to sustain breast cancer stem cells.* Genes Dev, 2015. **29**(1): p. 1-6.
61. Tagliabue, E., C. Ghirelli, P. Squicciarini, P. Aiello, M.I. Colnaghi, and S. Menard, *Prognostic Value of a6B4 Integrin expression in breast carcinomas is affected by laminin production from Tumor cells.* Clinical Cancer Research, 1998. **4**: p. 407-410.
62. Liang, J., S. Zheng, X. Xiao, J. Wei, Z. Zhang, I. Ernberg, L. Matskova, G. Huang, and X. Zhou, *Epstein-Barr virus-encoded LMP2A stimulates migration of nasopharyngeal carcinoma cells via EGFR/Ca2+/calpain/ITGβ4 axis.* Biol Open, 2017.
63. Kim, H.-D., F.B. Gertler, T.W. Guo, A.P. Wu, A. Wells, and D.A. Lauffenburger, *Epidermal Growth Factor–induced Enhancement of Glioblastoma Cell Migration in 3D Arises from an Intrinsic Increase in Speed But an Extrinsic Matrix and Proteolysis-dependent Increase in Persistence.* Molecular Biology of the Cell, 2008. **19**: p. 4249-4259.

64. Rojas, M., S. Yao, and Y.-Z. Lin, *Controlling Epidermal Growth Factor (EGF)-stimulated Ras Activation in Intact Cells by a Cell-permeable Peptide Mimicking Phosphorylated EGF Receptor.* J Biol Chem, 1996. **271**(44): p. 27456-27461.
65. Fincham, V.J., M. James, M.C. Frame, and S.J. Winder, *Active ERK/MAP kinase is targeted to newly forming cell-matrix adhesions by integrin engagement and v-SRC.* The EMBO Journal, 2000. **19**(12): p. 2911-2923.
66. Platt, M.O., A.J. Roman, A. Wells, D.A. Lauffenburger, and L.G. Griffith, *Sustained epidermal growth factor receptor levels and activation by tethered ligand binding enhances osteogenic differentiation of multi-potent marrow stromal cells.* J Cell Physiol, 2009. **221**(2): p. 306-17.
67. Leloup, L., H. Shao, Y.H. Bae, B. Deasy, D. Stolz, P. Roy, and A. Wells, *m-Calpain activation is regulated by its membrane localization and by its binding to phosphatidylinositol 4,5-bisphosphate.* J Biol Chem, 2010. **285**(43): p. 33549-66.
68. Glading, A., F. Uberall, S.M. Keyse, D.A. Lauffenburger, and A. Wells, *Membrane proximal ERK signaling is required for M-calpain activation downstream of epidermal growth factor receptor signaling.* J Biol Chem, 2001. **276**(26): p. 23341-8.
69. Chan, K.T., D.A. Bennin, and A. Huttenlocher, *Regulation of adhesion dynamics by calpain-mediated proteolysis of focal adhesion kinase (FAK).* J Biol Chem, 2010. **285**(15): p. 11418-26.
70. Franco, S., B. Perrin, and A. Huttenlocher, *Isoform specific function of calpain 2 in regulating membrane protrusion.* Exp Cell Res, 2004. **299**(1): p. 179-87.
71. Li, C.L., D. Yang, X. Cao, F. Wang, D.Y. Hong, J. Wang, X.C. Shen, and Y. Chen, *Fibronectin induces epithelial-mesenchymal transition in human breast cancer MCF-7 cells via activation of calpain.* Oncol Lett, 2017. **13**(5): p. 3889-3895.
72. Storr, S.J., K.W. Lee, C.M. Woolston, S. Safuan, A.R. Green, R.D. Macmillan, A. Benhasouna, T. Parr, I.O. Ellis, and S.G. Martin, *Calpain system protein expression in basal-like and triple-negative invasive breast cancer.* Ann Oncol, 2012. **23**(9): p. 2289-96.
73. Mamoune, A., J.-H. Luo, D.A. Lauffenburger, and A. Wells, *Calpain-2 as a Target for Limiting Prostate Cancer Invasion.* Cancer Res, 2003. **63**: p. 4632-4640.

Supporting Materials

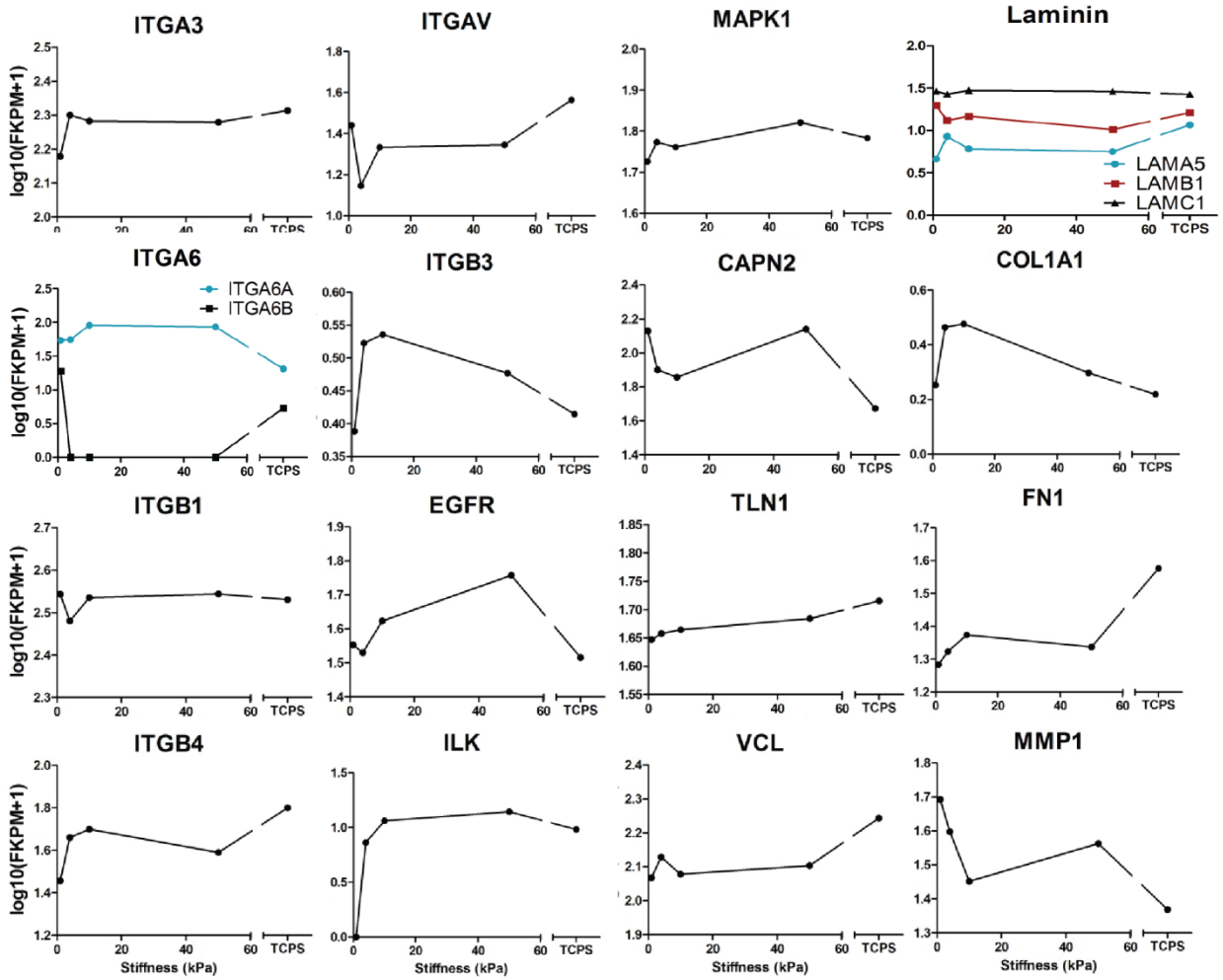

Supplemental Figure 1. RNA-Seq implicates several integrin-signaling related mechano-sensitive genes Genes related to ECM, integrins and downstream signaling identified from RNA-Seq performed on MDA-MB-231 cells cultured on 2D PEG-PC gels after 24 hours or lysed directly from TCPS. Gene names are given above each plot, with different isoforms (if applicable) as different colored lines. The y-axis is expression (log 10 scale) and the x-axis denotes the different stiffnesses of gel upon which cells were cultured (+ the TCPS comparison as a very stiff control). Genes identified are: integrin α_3 (ITGA3), integrin α_6 (ITGA6 with A and B isoforms), integrin β_1 (ITGB1), integrin β_4 (ITGB4), integrin α_v (ITGAV), integrin β_3 (ITGB3), epidermal growth factor receptor (EGFR), integrin-linked kinase (ILK), mitogen-activated protein kinase 1 (MAPK1), calpain 2 (CAPN2), talin 1 (TLN1), vinculin (VCL), laminin (LAM, A5, B1, C1 isoforms), collagen 1A1 (COL1A1), fibronectin 1 (FN1), and matrix metalloproteinase 1 (MMP1).

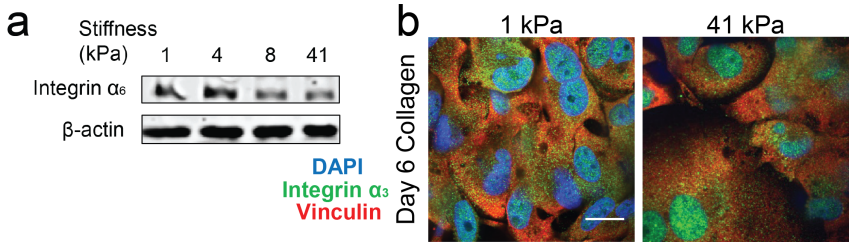

Supplemental Figure 2. Cells express integrin α_6, but not α_3 in a stiffness-sensitive manner. (a) Protein expression of integrin α_6 in MDA-MB-231 cells determined via western blot. Cells were cultured on gels or 1, 4, 8, and 41 kPa for 24 hours before lysis and blotting. (b) MDA-MB-231 cells were cultured on gels of 1 or 41 kPa functionalized with 10 μg cm^{-2} for 6 days before fixing. Cells were stained for vinculin (red) and integrin α_3 (green) and nuclei were labeled with DAPI (blue). Scale bar = 20 μm.

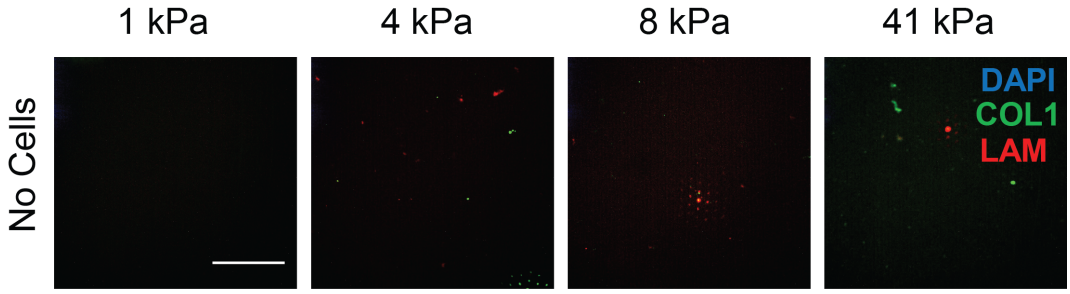

Supplemental Figure 3. Media changes do not result in deposited matrix. 2D PEG-PC gels were protein coated with 10 μg cm^{-2} collagen 1, but no cells were seeded on the gels. Media containing 10% FBS was changed every 2 days for 6 days. Gels were then fixed and stained collagen 1 (green) and laminin (red), and nuclei were labeled with DAPI. Scale bar = 100 μm.

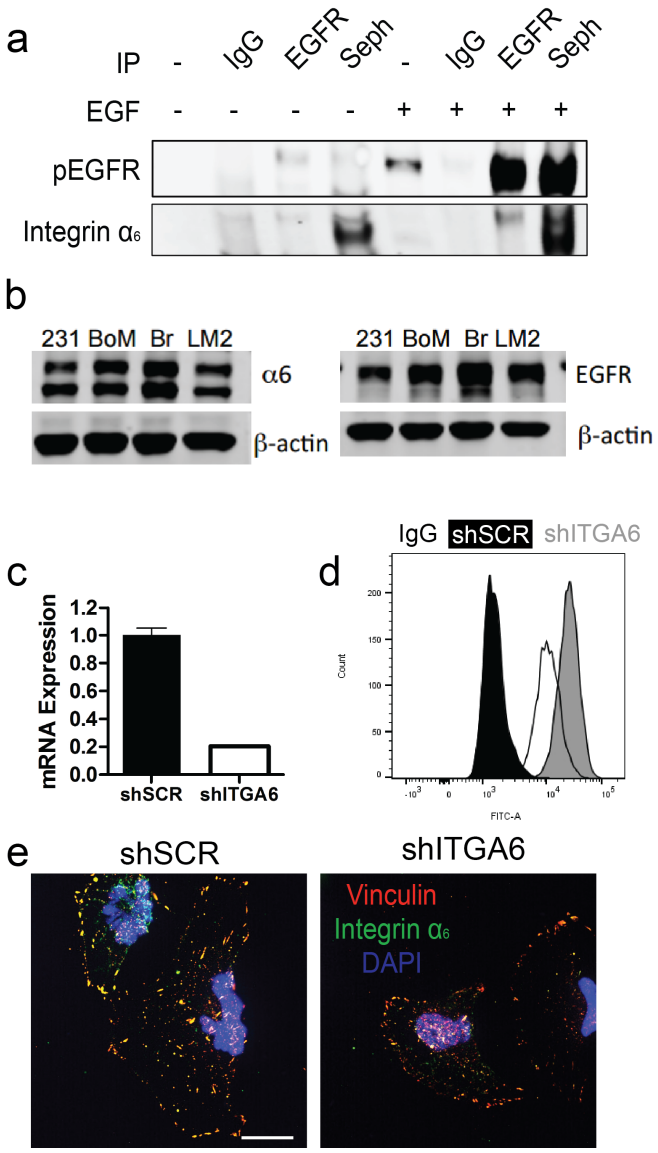

Supplemental Figure 4. Extension of cell assays and the PEG-PC material system. (a) Co-immunopreciptation of EGFR and integrin α_6 either without EGF (-) or with EGF (+). Lysates were pulled down with Rabbit IgG and agarose protein A beads (IgG), EGFR antibody with agarose protein A beads (EGFR), or with sepharose beads with pre-conjugated EGFR antibody (Seph). (b) Western blot of integrin α_6 and EGFR from parental MDA-MB-231 cells (231), and cells selected for tissue specific metastasis to the bone (BoM), brain (br), or lung (LM2) by the Massague group, assayed on TCPS (Bos et al. 2009; Kang et al. 2003; Minn et al. 2005). (c) mRNA expression of integrin α_6 determined via qRT-PCR in integrin α_6 knockdown cells (shTGA6) and scramble control (shSCR). Data is normalized to shSCR cells. (d) Surface expression (determined by FACS) of scramble control and shITGA6 knockdown cells. (e) Permeabilizing the cell membrane before fixing and immunofluorescent staining confirmed that there is less integrin α_6 associated with focal adhesions in the knockdown cells compared to a scramble shRNA control. Cells were immunofluorescently stained for insoluble vinculin (red), insoluble integrin α_6 (green) and DAPI (blue).

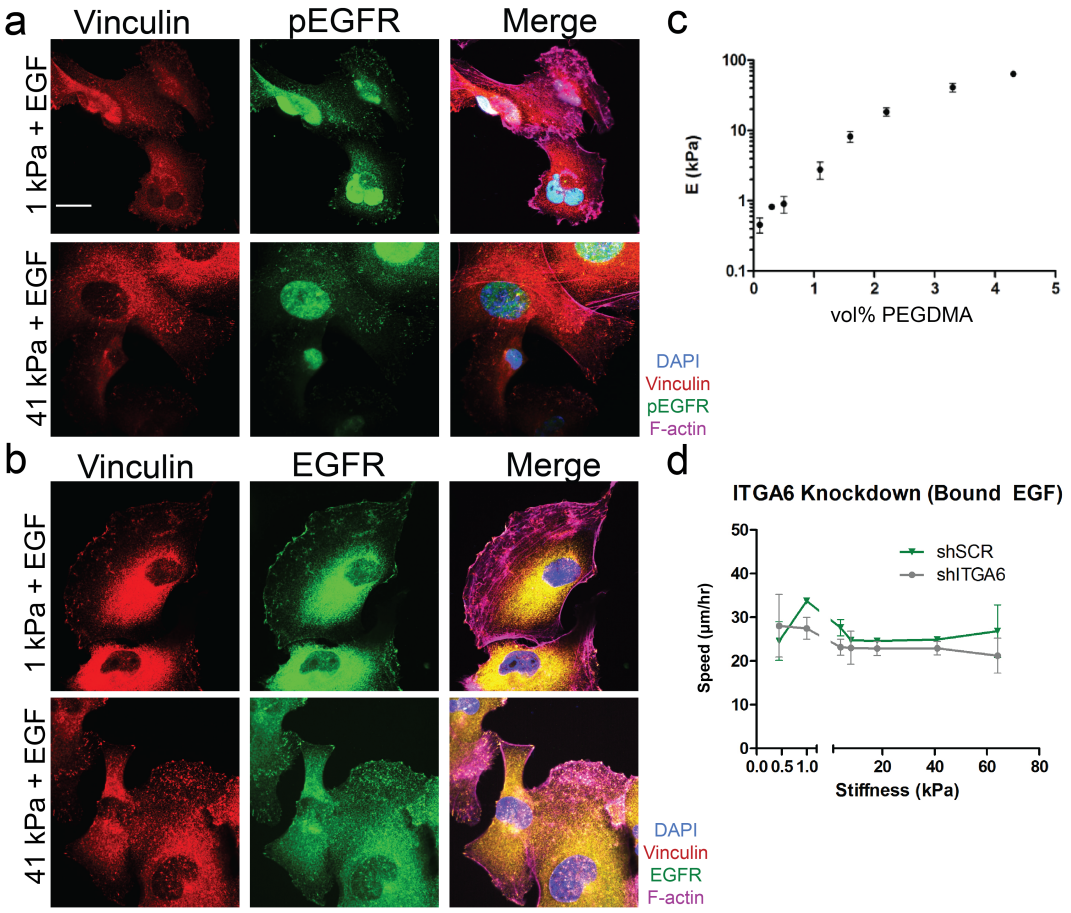

Supplemental Figure 5. Total EGFR and pEGFR(y1068) is present at focal adhesions in the presence of EGF ligated to the surface (a-b) Immunofluorescence of cells seeded on 1 or 41 kPa gels, with 10 μg cm^{-2} collagen 1 and 20 ng cm^{-2} bound EGF for 24 hours. Cells were stained for vinculin (red), pEGFR(pY1068) (in (a), green), phalloidin (purple), and DAPI (blue) (a) or vinculin (red), total EGFR (in (b), green), phalloidin (purple), and DAPI (blue) (b). Scale bar = 20 μm. (d) The compressive Young's modulus of PEG-PC hydrogels, as a function of vol% of PEGDMA. This range is expanded from (Herrick et al. 2013). (d) Migration speeds of integrin α_6 knockdown cells (ITGA6) and scramble control cells (shSCR) in the presence of 10 μg cm^{-2} collagen 1 and 20ng cm^{-2} EGF bound to the gel.

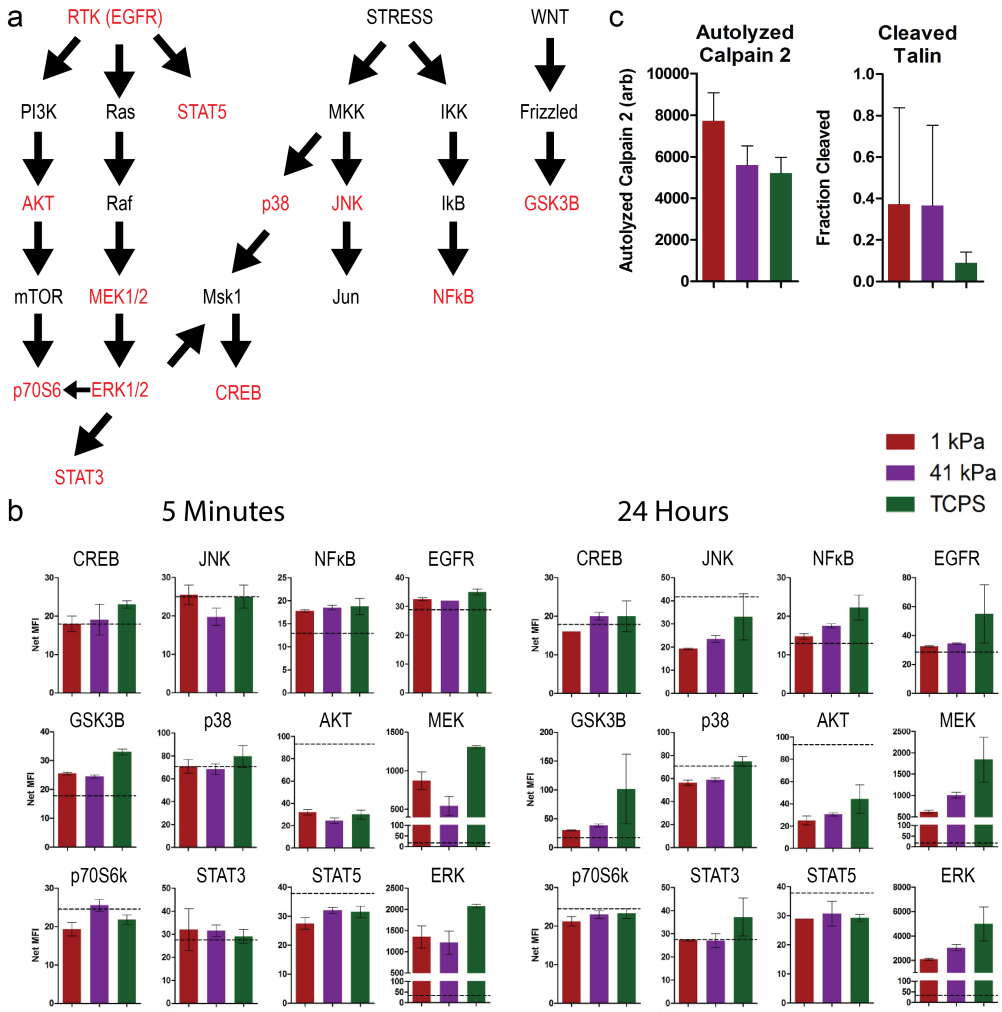

Supplemental Figure 6. Bead-based ELISA and Western Blotting used to quantify signaling during cell adhesion in the presence of mechanical and biochemical stimuli. (a) Signaling diagram of analytes quantified across several integrin- and growth factor-related pathways. (b) Luminex bead-based ELISA of CREB (pS133), JNK (pT183/pY185), NFκB (pS536), EGFR (pan-Tyr), GSK3B (pS9), p38 (pT180/pY182), AKT (pS473), MEK (pS222), p70S6k (pT412), STAT3 (pS727), STAT5 (pY694/699), and ERK (pT185/pY187) during adhesion to TCPS or gels of 1 or 41 kPa with 10μg cm^{-2} collagen 1 on the surface. Both the suspended and adhered fractions were collected at 5 minutes. (c) Western blot was used to quantify autolyzed calpain 2 and cleaved talin.

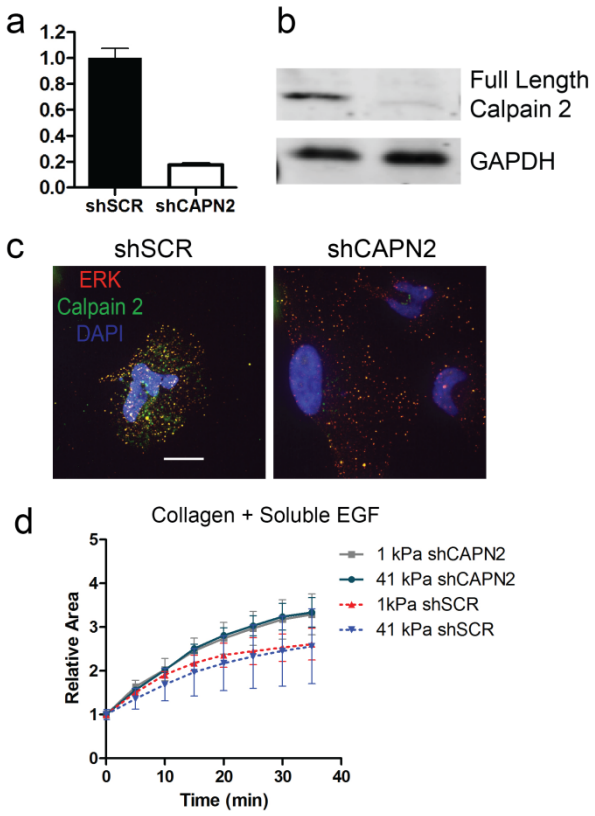

Supplemental Figure 7. Knockdown of calpain 2 limits response to EGF on hydrogels. (a-b) mRNA expression (a; determined via qRT-PCR) and protein expression (b; determined by western blot) of scramble control and shCAPN2 knockdown cells. (c) Permeabilizing the cell membrane before fixing and immunofluorescent staining confirmed that there is less calpain 2 associated with focal adhesions in the knockdown cells compared to a scramble shRNA control. Cells were immunofluorescently stained for insoluble ERK (red), insoluble calpain 2 (green) and DAPI (blue). (d) shCAPN2 cells are less responsive to EGF during adhesion than the shSCR control cells. All area measurements are normalized to time 0.

Table S1. RT-PCR Primers used for gene expression quantification.

Gene	Accession number	position	Forward sequence, 5'-3'	position	Reverse sequence, 5'-3'
ITGA3	NM_002204.3	4451	TCTCTCCTTGGCCACAGACT	4655	TTCTGAGGCTGGCTGGTAGT
ITGA6	NM_000210.3	747	TTGGAGCTTTTGTGATGGGC	967	GCTCAGTCTCTCCACCAACT
ITGB1	NM_002211.3	2054	CATCTGCGAGTGTGGTGTCT	2262	GGGGTAATTTGTCCCGACTT
ITGB4	NM_000213.3	2946	ACTACACCCTCACTGCAGAC	3154	TCTGGCTTGCTCCTTGATGA
EGFR	NM_005228.3	1728	AGGTGAAAACAGCTGCAAGG	1957	AGGTGATGTTCATGGCCTGA
CAPN2	NM_001748.4	1533	CCAGAGGAGTTAAGTGGGCA	1733	AGAAAAGACCCGGATGCAGA
MMP-1	NM_002421.3	739	AAGATGAAAGGTGGACCAACAATT	817	CCAAGAGAATGGCCGAGTTC
Talin 1	NM_006289.3	351	CACCATGGTTGCACTTTCAC	582	CCCATTTCGGAGCATGTAGT
Vinculin	NM_014000.2	3203	GCCAAGCAGTGCACAGATAA	3387	AGGTTCTGGGCATTGTGAAC
MAPK1	NM_002745.4	766	CCAGACCATGATCACACAGG	928	CTGGAAAGATGGGCCTGTTA
RPS-13	NM_001017	217	AAGTACGTTTTGTGACAGGCA	403	CGGTGAATCCGGCTCTCTATTAG
β-actin	NM_001101	747	GGACTTCGAGCAAGAGATGG	980	AGCACTGTGTTGGCGTACAG

References

Bos, P. D., X. H. Zhang, C. Nadal, W. Shu, R. R. Gomis, D. X. Nguyen, A. J. Minn, M. J. van de Vijver, W. L. Gerald, J. A. Foekens, and J. Massague. 2009. 'Genes that mediate breast cancer metastasis to the brain', *Nature*, 459: 1005-9.

Herrick, W. G., T. V. Nguyen, M. Sleiman, S. McRae, T. S. Emrick, and S. R. Peyton. 2013. 'PEG-phosphorylcholine hydrogels as tunable and versatile platforms for mechanobiology', *Biomacromolecules*, 14: 2294-304.

Kang, Yibin, Peter M. Siegel, Weiping Shu, Maria Drobnjak, Sanna M. Kakonen, Carlos Cordón-Cardo, Theresa A. Guise, and Joan Massagué. 2003. 'A multigenic program mediating breast cancer metastasis to bone', *Cancer Cell*, 3: 537-49.

Minn, A. J., G. P. Gupta, P. M. Siegel, P. D. Bos, W. Shu, D. D. Giri, A. Viale, A. B. Olshen, W. L. Gerald, and J. Massague. 2005. 'Genes that mediate breast cancer metastasis to lung', *Nature*, 436: 518-24.